Int. J. Solids Structures, 1965, Vol. 1, pp. 179 to 188. Pergamon Press Ltd. Printed in Great Britain

APPLICATION OF THE SLAB ANALOGY TO THE STUDY OF STRESS FIELDS INDUCED BY IMPERFECTIONS IN CRYSTALS

T. MURA, A. OTSUKA

Department of Civil Engineering and Materials Research Center, Northwestern University, Evanston

and

O. C. ZIENKIEWICZ

Department of Civil Engineering, University College of Swansea

Abstract—Two-dimensional stress fields in crystals due to edge dislocations, vacancies, precipitations, cracks and their combinations are obtained experimentally by using the slab analogy between an Airy stress function in a slice and a deflection in a slab. The results agree fairly well with those obtained theoretically. It is thus found that some complicated problems in stress analysis in the field of micromechanics can be solved with the method proposed in this paper.

1. INTRODUCTION

THE slab analogy was first recognized by Timpe [1] in 1905. The practical applications of the analogy to stress analysis were not found until 1908 by Wieghardt [2] and 1931 by Jensen [3]. Some improvements in the techniques were introduced by Crantz [4] in 1939 by adopting Einsporn's optical spherometer for measuring the curvature of the deflected plate. Details of the mathematics were developed by Mindlin [5] in 1946, and by Mindlin and Salvadori [6] in 1954. Zienkiewicz and Cruz [7] and later Bouwkamp [8] recognized the advantages of using the Moiré method in applying the analogy and have shown how many problems of stress distribution can be solved simply. The Moiré method and its general technique of application to structural problems is described by Ligtenberg [9] and Bradley [10].

In this paper, the slab analogy will be applied to the recently developing field of mechanics related to the microstructure of materials. The stress fields due to dislocations, precipitations, inclusions and microcracks in crystals are obtained from the Moiré fringes in photographs taken by reflecting light between the grid screen and the slab surface. Some of the results are compared with the theoretical solutions obtained by the theory of elasticity. This is a new application of the slab analogy to the study of stress fields induced by impurities in crystals. Although the problem can be solved numerically with the aid of a computer, this paper presents an alternative which has some practical advantages in as much as the configuration can be easily changed and a full visual picture of the stress variation is easily obtained.

2. SLAB ANALOGY

The theory of the slab analogy presented here is an extension and reformulation somewhat following the lines of reference [6] and earlier works in this area. The derivation is simplified by introducing the tensor notation.

Let us consider a two-dimensional domain of a crystal bounded by c_0 (Fig. 1(a)). The problem is to find the stress field when a dislocation is given inside c and a boundary force X_i is given on c_0. The stress field can be obtained from the curvature of deflection of the slab, (Fig. 1(b)), by applying a suitable transverse load and moments inside c' with suitable constraint conditions on c'_0. The slab has a geometrical symmetry with the domain of the crystal. The two-dimensional domain of the crystal will be called 'slice' hereafter. The Cartesian coordinates (x_i) and (x'_i) are introduced in the slice and the slab, respectively.

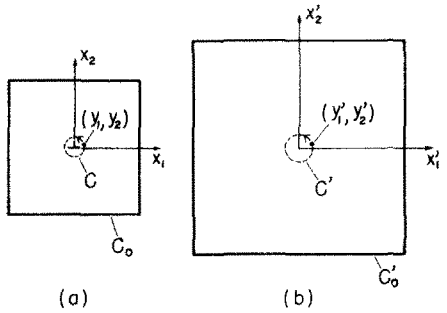

FIG. 1. Illustration of two-dimensional domains of slice (a) and slab (b).

The following line integrals of the increment of displacement, dU_i, and the increment of rotation about the x_3-axis, $d\omega_3$, are the fundamental formulae in the slice [6]:

$$\begin{aligned} \oint_c d\omega_3 &= \oint_c e_{3_{ij}} \varepsilon_{jk,i}\, dx_k, \\ \oint_c dU_i &= \oint_c \varepsilon_{ij}\, dx_j + \oint_c e_{3_{ih}} x_h e_{3_{lj}} \varepsilon_{jk,l}\, dx_k - e_{3_{ij}} y_j \oint_c d\omega_3, \end{aligned} \tag{1}$$

where c is the Burgers circuit of the integration, ε_{ij} a strain tensor, $e_{3_{ij}}$ a unit permutation tensor, and y_j is a coordinate of a starting point of circuit c.

If the strain tensor in (1) is expressed by an Airy stress function, φ, by using Hooke's law, (1) can be written as follows for the plane state of stress:

$$\begin{aligned} \oint_c d\omega_3 &= \frac{1}{E} \oint_c \frac{\partial}{\partial n} (\nabla^2 \varphi)\, ds, \\ \oint_c dU_i + e_{3_{ij}} y_j \oint_c d\omega_3 &= \frac{1}{E} \oint_c \left(e_{3_{ij}} x_j \frac{\partial}{\partial n} (\nabla^2 \varphi) - x_i \frac{\partial}{\partial s} (\nabla^2 \varphi) \right) ds - \frac{1+\nu}{E} \oint_c \frac{\partial}{\partial s} (\varphi_{,i})\, ds, \end{aligned} \tag{2}$$

where dn and ds are the normal and the tangential line element on circuit c, and E and ν are Young's modulus and Poisson's ratio, respectively. The corresponding expression for plane strain is obtained by replacing the factor $(1/E)$ in (2) by $(1-\nu^2)/E$.

Considering the analogous slab (Fig. 1(b)), let F_3 and T_i represent, respectively, the resultants of forces and couples acting on the region within c' referring to point y_i', where y_i' is a coordinate of a starting point of circuit c'. Then F_3 and T_i can be written in terms of shear force Q_i and moment M_{ij} defined on c' as follows:

$$\begin{aligned} F_3 &= -\oint_{c'} Q_i n_i \, \mathrm{d}s, \\ T_i &= -\oint_{c'} e_{3_{ij}}(x_j'-y_j')Q_k n_k \, \mathrm{d}s + \oint_{c'} e_{3_{ij}} M_{jk} n_k \, \mathrm{d}s, \end{aligned} \tag{3}$$

where n_i is the normal vector on circuit c'. M_{ij} and Q_i can also be written in terms of the deflections of the slab, w, as follows:

$$\begin{aligned} M_{ij} &= D(1-\nu')w_{,ij} + \delta_{ij} D\nu' \nabla^2 w, \\ Q_i &= M_{ij,j}, \end{aligned} \tag{4}$$

where D and ν' are the bending rigidity and Poisson's ratio, respectively. Substituting (4) into (3) leads to

$$\begin{aligned} F_3 &= -D \oint_{c'} \frac{\partial}{\partial n}(\nabla^2 w) \, \mathrm{d}s, \\ T_i + e_{3_{ij}} y_j' F_3 &= -D \oint_{c'} \left(e_{3_{ij}} x_j' \frac{\partial}{\partial n}(\nabla^2 w) - x_i' \frac{\partial}{\partial s}(\nabla^2 w) \right) \mathrm{d}s + D(1-\nu') \oint_{c'} \frac{\partial}{\partial s}(w_{,i}) \, \mathrm{d}s. \end{aligned} \tag{5}$$

For the slab analogy to be valid we can take

$$\begin{aligned} \varphi &= \gamma \lambda^2 w, \\ \mathrm{d}x_i &= \lambda \, \mathrm{d}x_i', \end{aligned} \tag{6}$$

with the coefficients of proportionality, λ and γ. Now, substituting (6) into (5) and comparing the result with (2) leads to

$$\begin{aligned} -\frac{\gamma F_3}{D} &= E \oint_c \mathrm{d}\omega_3, \\ -\frac{\gamma \lambda}{D}(T_i + e_{3_{ij}} y_j' F_3) &= E\left(\oint_c \mathrm{d}U_i + e_{3_{ij}} y_j \oint_c \mathrm{d}\omega_3 \right) + (\nu+\nu') \oint_c \frac{\partial}{\partial s}(\varphi_{,i}) \, \mathrm{d}s. \end{aligned} \tag{7}$$

Now if $\oint_c \mathrm{d}U_i$ and $\oint_c \mathrm{d}\omega_3$ are made proportional to T_i and F_3, respectively, and if $\oint_c \frac{\partial}{\partial s}(\varphi_{,i}) \, \mathrm{d}s$ is zero (the requirement of a zero force resultant on such a region) then the analogy is satisfied.

The deflection of the slab, however, is under the following constraint conditions on c_0':

$$\begin{aligned} \gamma w &= \frac{1}{\lambda^2} \int_0^s A_i n_i \, \mathrm{d}s, \\ \gamma \frac{\partial w}{\partial n} &= -\frac{1}{\lambda} A_i \frac{\mathrm{d}x_i'}{\mathrm{d}s}, \end{aligned} \qquad \text{on } c_0' \tag{8}$$

where

$$A_i = \int_0^s X_i \, ds, \tag{9}$$

which imposes prescribed deflections and slopes on the boundary. It should be noted that if the boundary, c_0, in the slice is free from surface tractions, the corresponding boundary, c_0' in the slab becomes a clamped edge. If the stress field in the slice is due to an edge dislocation with Burgers vector b in the x_1-direction, we take $\oint_c dU_1 = b$, $\oint_c dU_2 = 0$, $\oint_c d\omega_3 = 0$ and $\oint_c \frac{\partial}{\partial s}(\varphi_{,i})\, ds = 0$. The mean radius of c in this case can be assumed to be infinitely small. It can be seen from (6) and (7) that the stress field can be obtained from the deflection field of the slab by applying a concentrated couple, T_1, which is proportional to the Burgers vector. If the c in the slice is a boundary of a crack or a vacancy, the corresponding domain bounded by c' in the slab can be replaced by a rigid plug without F_3 and T_i. When the slice has an edge dislocation and a crack, the slab analogy can be achieved by applying a concentrated couple at the corresponding dislocation position in the slab which has a rigid plug or domain corresponding to the domain of the crack in the slice.

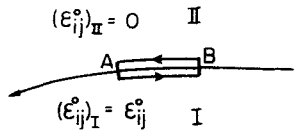

FIG. 2. Illustration of a discontinuity line c and a path of the line integral.

As a further application of the slab analogy, it will be interesting to show the stress field due to a coherent precipitation in crystals. The stress field can be regarded as the residual stress field due to an initial strain distributed as ε^0_{ij} = constant inside of c and $\varepsilon^0_{ij} = 0$ outside of c. It can be seen from (1) that the residual stress field is equivalent to the stress field due to a surface dislocation distributed along c. Since ε_{ij} in (1) is the sum of an elastic strain and the initial strain ε^0_{ij}, integrals

$$\left[-\oint_c e_{3ij} \varepsilon^0_{jk,i} \, dx_k \right] \text{ and } \left[-\oint_c \varepsilon^0_{ij} \, dx_j - \oint_c e_{3ih} x_h e_{3lj} \varepsilon^0_{jk,l} \, dx_k \right]$$

take the places of $\oint_c d\omega_3$ and $\oint_c dU_i$ in (1), provided that there are no dislocations. If the path c is taken as a narrow strip AB in domain I and BA in domain II as shown in Fig. 2, the former becomes zero and the latter becomes

$$\left[-\left(\int_A^B (\varepsilon^0_{ij})_I \, dx_j + \int_B^A (\varepsilon^0_{ij})_{II} \, dx_j \right) = \int_B^A \varepsilon^0_{ij} \, dx_j \right]$$

Replacing $\oint dU_i$ in (7) by $\oint_c \varepsilon^0_{ij} \, dx_j$, and putting $\oint_c d\omega_3 = 0$, $\oint_c \frac{\partial}{\partial s}(\varphi_{,i})\, ds = 0$ one obtains

$$\begin{aligned} -\frac{\gamma\lambda F_3}{D} &= 0, \\ -\frac{\gamma\lambda T_i}{D} &= E \oint_c \varepsilon^0_{ij} \, dx_j. \end{aligned} \tag{10}$$

It can be regarded as a line distribution of moment along c' with t_i satisfying the relation

$$-\frac{\gamma t_i}{D} = E\varepsilon_{ij}^0 \frac{dx_j'}{ds}. \tag{11}$$

3. EXPERIMENTS

A square slab ($12'' \times 12'' \times \frac{1}{8}''$) of Plexiglas (P in Fig. 3) is clamped in a steel frame and set parallel to a grid screen (S in Fig. 3). A camera is mounted behind a hole in the center of the screen. The front surface of the slab reflects the image of the grid screen into the camera. The film is exposed first to the grid screen image reflecting from the undeformed slab, and then to the image reflecting from the deformed slab. The resulting double exposure consists of Moiré fringes, which are related to the deflection of the slab. The black spot near the centers of the pictures is an image of the camera hole in the grid screen. The cross lines passing through the image of the camera hole are caused by slight mismatches in jointing the four pieces of grid paper on the screen.

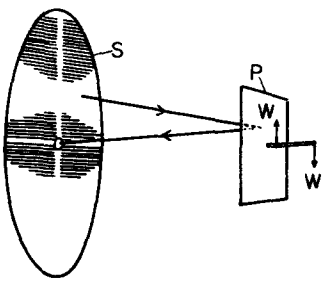

FIG. 3. Illustration of the circular grid screen (S), the slab of Plexiglas (P), and the loads (w).

(a) *An edge dislocation*

An edge dislocation in the slice corresponds simply to one concentrated couple on the slab. The couple is applied by a Plexiglas bar carrying two opposite loads. The bar is attached by suitable cement at the position corresponding in the slab to the position of dislocation in the slice.

The mathematical expression of the stress field of the dislocation is

$$\begin{aligned} \sigma_x &= -\frac{Gb}{2\pi(1-\nu)} \frac{y(3x^2+y^2)}{(x^2+y^2)^2}, \\ \sigma_y &= \frac{Gb}{2\pi(1-\nu)} \frac{y(x^2-y^2)}{(x^2+y^2)^2}, \end{aligned} \tag{12}$$

when the material is infinitely extended.

Figure 4 and Fig. 6 are the photographs of the fringes for this case. In Fig. 4 the direction of the lines of the grids is parallel to the x-axis. In Fig. 6 the direction of the lines of the grids is normal to the x-axis. Figs. 5 and 7 show their stress fields. The theoretical values are calculated from the above formula by neglecting the edge effect of the slice.

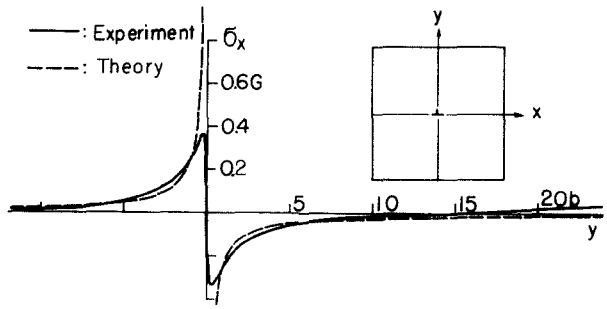

FIG. 5. Experimental value of σ_x calculated from Fig. 4 along the y-axis, comparing with the well-known solution (A. H. Cottrell, *Plastic Flow in Crystals*, p. 34) in an infinitely extended material. b is the Burgers vector and G is the shear modulus.

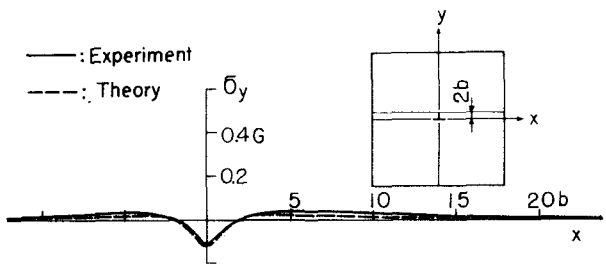

FIG. 7. Experimental value of σ_y calculated from Fig. 6 along the $y = 2b$ line, comparing with the well-known solution (A. H. Cottrell, *Plastic Flow in Crystals*, p. 34) in an infinitely extended material.

(b) *A circular precipitation*

Precipitation in the slice corresponds to a distributed torque applied along the closed line in the slab which corresponds to the boundary of precipitation in the slice.

The distributed torque is applied to the boundary by bending of a series of bars which are attached to the slab. The theoretical stress field of a circular disk of radius b due to a uniform dilatation $\varepsilon_{ij}^0 = \delta_{ij}\varepsilon_0$ inside of a circular disk with radius a can be obtained from "Theory of Elasticity" by Timoshenko, p. 407, and gives

$$\begin{aligned}
\sigma_r &= \tfrac{1}{2}\varepsilon_0 E\frac{a^2}{b^2}\left(1-\frac{b^2}{r^2}\right) && \text{for } r \geq a \\
&= \tfrac{1}{2}\varepsilon_0 E\frac{a^2}{b^2}\left(1-\frac{b^2}{a^2}\right) && \text{for } r \leq a, \\
\sigma_\theta &= \tfrac{1}{2}\varepsilon_0 E\frac{a^2}{b^2}\left(1+\frac{b^2}{r^2}\right) && \text{for } r \geq a \\
&= \tfrac{1}{2}\varepsilon_0 E\frac{a^2}{b^2}\left(1-\frac{b^2}{a^2}\right) && \text{for } r \leq a.
\end{aligned} \tag{13}$$

We assume this stress field is the same stress field as that due to a circular precipitate with radius a. Figure 8 shows the photograph of Moiré fringes of the slab, when the

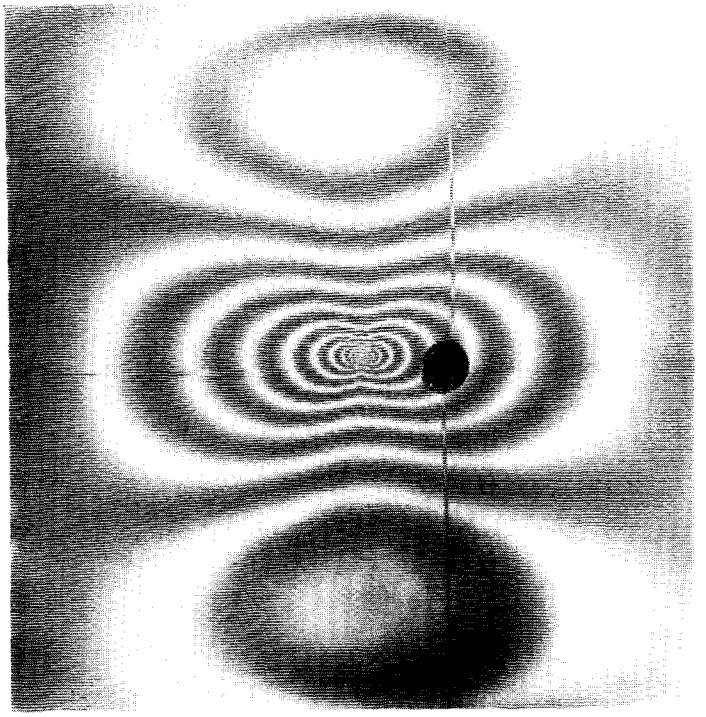

FIG. 4. Moiré fringes showing white contour lines of $\partial w/\partial y$ in the slab, corresponding to $\partial\varphi/\partial y$ in the stress field due to an edge dislocation located at the center of the slice.

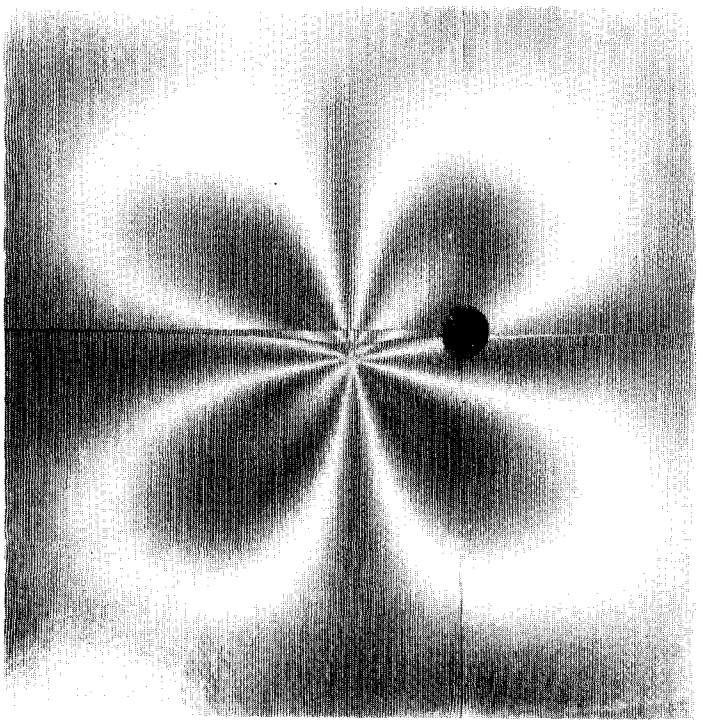

FIG. 6. Moiré fringes showing white contour lines of $\partial w/\partial x$ in the slab, corresponding to $\partial\varphi/\partial x$ in the stress field due to an edge dislocation located at the center of the slice.

[*facing p. 184*

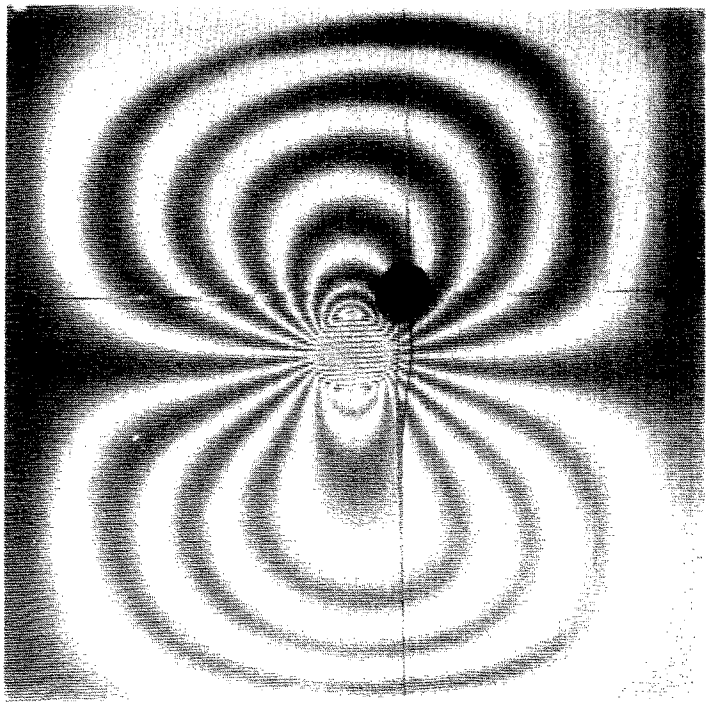

FIG. 8. Moiré fringes showing white contour lines of $\partial w/\partial y$, corresponding to $\partial \varphi/\partial y$ in the stress field due to a circular precipitation at the center of the slice.

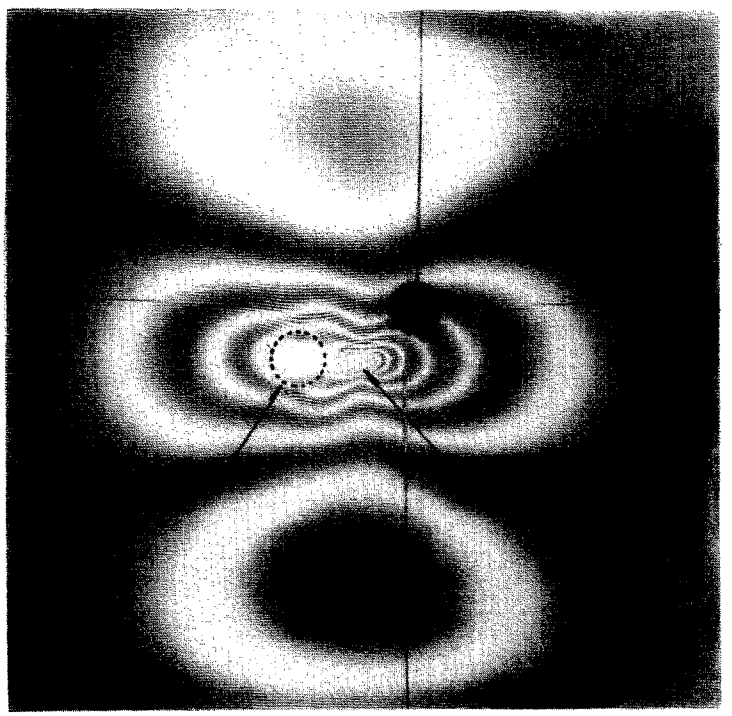

FIG. 10. Moiré fringes showing white contour lines of $\partial w/\partial y$, corresponding to $\partial \varphi/\partial y$ for the stress field in the neighborhood of a circular hole due to an edge dislocation.

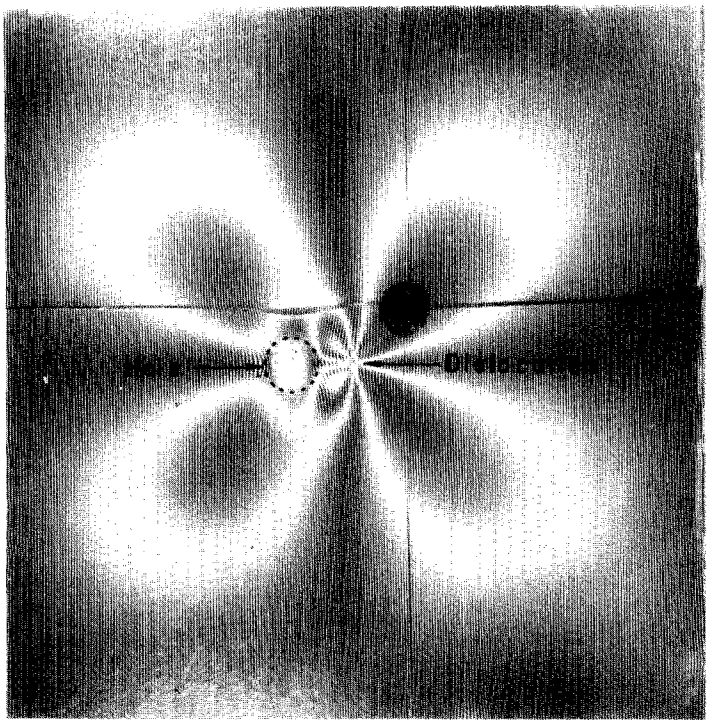

FIG. 12. Moiré fringes showing white contour lines of $\partial w/\partial x$, corresponding to $\partial\varphi/\partial x$ for the stress field in the neighborhood of a circular hole due to an edge dislocation.

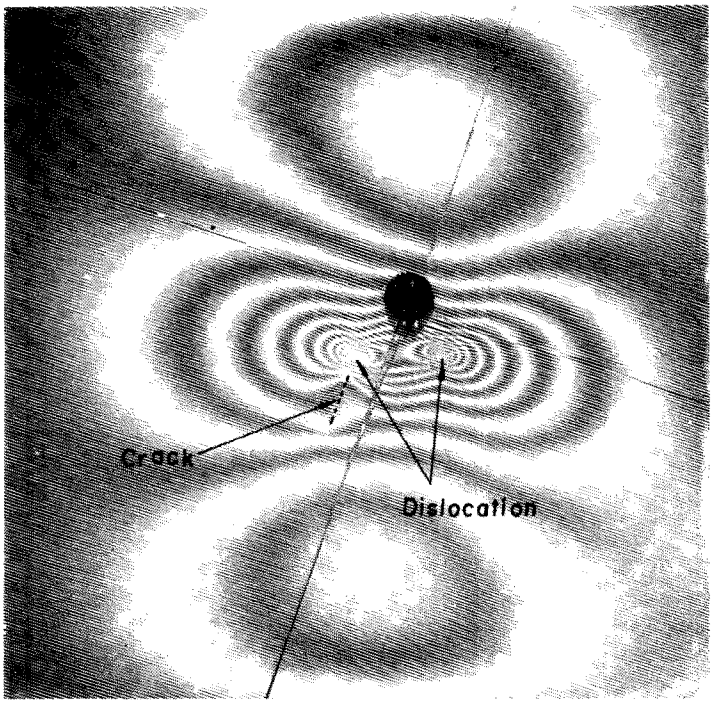

FIG. 13. Moiré fringes showing white contour lines of $\partial w/\partial y'$, corresponding to $\partial\varphi/\partial y'$ for the stress field in the neighborhood of a crack due to two edge dislocations.

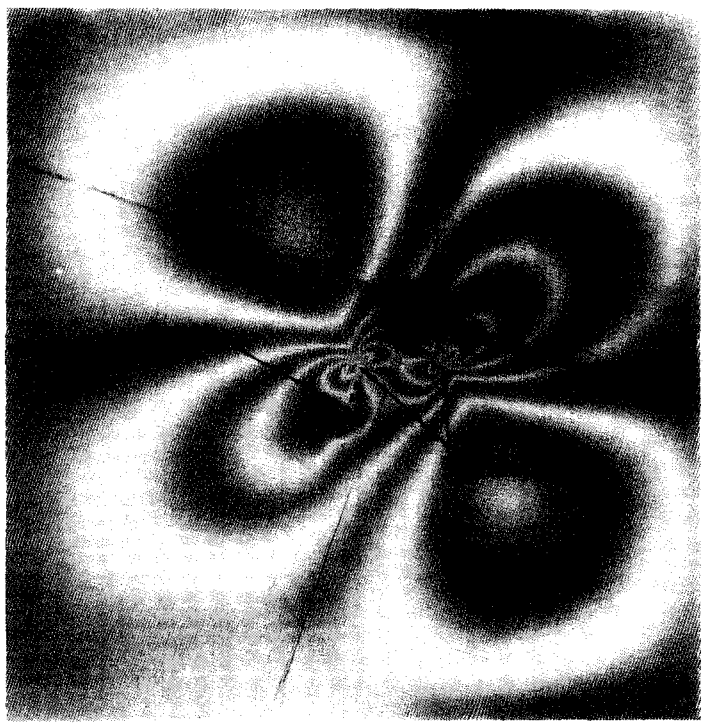

FIG. 15. Moiré fringes showing white contour lines of $\partial w/\partial x'$, corresponding to $\partial\varphi/\partial x'$ for the stress field in the neighborhood of a crack due to two edge dislocations.

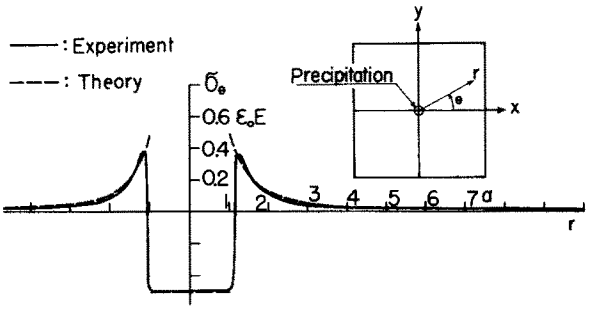

FIG. 9. Experimental values of σ_θ calculated from Fig. 8 along the y-axis, comparing with the well-known solution (S. Timoshenko, *Theory of Elasticity*, p. 407), where a is the radius of the precipitation, and ε_0 is the misfit strain.

lines of the grids are parallel to the x-axis. Figure 9 compares the stress distribution calculated by the slab analogy to the above theoretical field.

(c) *A dislocation and a circular hole*

In order to have a rigid domain in the slab corresponding to the hole in the slice, a circular cylinder of Plexiglas is attached at the position in the slab which corresponds to the hole in the slice, since the cylinder has an infinitely large rigidity of bending. An edge dislocation is located in the neighborhood of the hole. The mathematical solutions of this case is given by Dundurs and Mura [11]. Figures 10 and 12 show the Moiré fringes and Fig. 11 shows the stress distribution. The stress σ_y along the x-axis becomes zero.

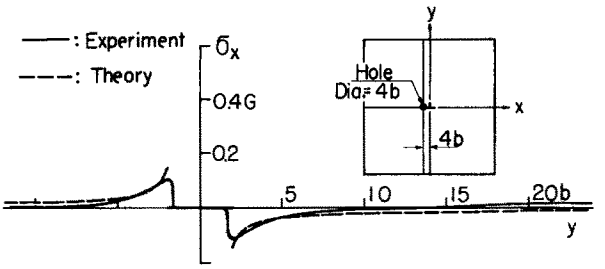

FIG. 11. Experimental value of σ_x calculated from Fig. 10 along the $x = -4b$ line, comparing with the solution by Dundurs and Mura [11].

(d) *A crack and two dislocations*

In order to have a rigid domain in the slab corresponding to the crack in the slice, a rectangular block of Plexiglas is attached at the corresponding position in the slab. The two dislocations are located in the neighborhood of the crack. The thickness of the crack is taken as that of the radius of the dislocation core. It means that the thickness of the rectangular block is comparable to the radius of the domain where the concentrated couple is applied.

The length of the crack is taken as four times of the dislocation core. The location of the crack is shown in Fig. 14. Figures 13 and 15 show the Moiré fringes when the

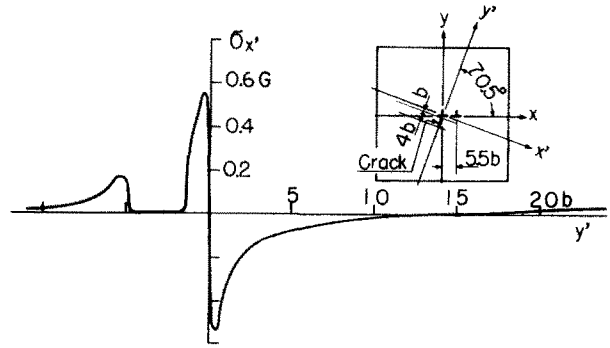

FIG. 14. Experimental value of $\sigma_{x'}$ calculated from Fig. 13 along the y'-axis.

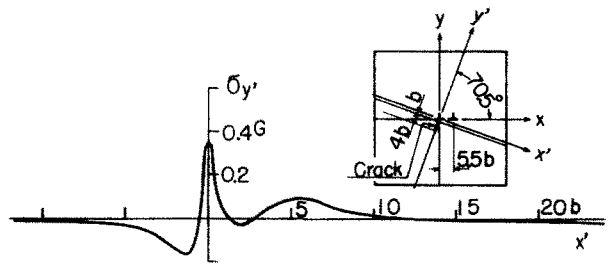

FIG. 16. Experimental value of σ_y calculated from Fig. 15 along the x'-axis.

grid lines are parallel to the x'-direction and the y'-direction, respectively. The experimental values of normal stress components along the x'- and y'-axes are shown in Fig. 14 and Fig. 16.

4. DISCUSSION

It is interesting to note in Fig. 5 that the value of the stress due to a dislocation has a finite maximum value about 0·4 G, contrary to the Volterra stress field (12) which becomes infinite at $y = 0$ when approached along the y-axis. This discrepancy stems from the fact that the concentrated couple in the analogy was applied at a certain finite domain in the slab instead of being applied at one point. Thus, the stress field obtained in this experiment can be understood as that of dislocations distributed inside the finite domain rather than that of a discrete dislocation at one point. As Peierls [12] pointed out, a more realistic state of the dislocation in crystals can be obtained by distributing infinitely small dislocations in a finite domain rather than a discrete dislocation at one point, where the total strength of the distributed dislocations is taken as the Burgers vector of the discrete dislocation. It is reasonable, therefore, to say that the stress field obtained in this experiment is closer to the stress field due to a Peierls dislocation, which is believed to be more realistic than the Volterra dislocation.

It can be seen from Fig. 6 that $\partial\varphi/\partial x$ is constant along the x-axis at $y = 0$. Since $\sigma_y = \partial^2\varphi/\partial x^2$, one obtains $\sigma_y = 0$ along the axis at $y = 0$, which agrees completely with (12).

The coefficients of proportionality λ and γ in (6) were taken as follows for Figs. 4–7. The radius ($\frac{1}{4}$ in.) of the domain in the slab where the concentrated couple was applied was assumed to correspond to the core radius or the Burgers vector ($b = 2{\cdot}86 \times 10^{-8}$ cm) of the dislocation. The ratio of the latter to the former yields $\lambda = 4{\cdot}5 \times 10^{-8}$. The value of γ is determined as $19{\cdot}3E$ cm from (7), $-\gamma\lambda T_1/D = Eb$, by substituting the applied couple $T_1 = -2{\cdot}946$ kg. cm, $b = 2{\cdot}86 \times 10^{-8}$ cm, and $D = 89{\cdot}6$ kg. cm.

It can be seen from Fig. 8 that $\partial^2\varphi/\partial y^2 = \sigma_x$ is constant along the y-axis inside the precipitation. Since σ_x along the y-axis is σ_θ, the distribution becomes as shown in Fig. 9. The position r along the y-axis is expressed in terms of the radius of the precipitation. The diameter of the precipitation corresponds to 1·2 in. diameter of the circular domain in the slab along which the line moment was applied. The coefficients λ and γ in this case were taken from (6) and (11) as $0{\cdot}656\,a$/cm and $70{\cdot}5\,\varepsilon_0 E$ cm respectively. The result agrees very well with (13).

The precipitation considered in this example is a special case of general precipitations. Some incoherent precipitations in crystals have no misfit to the matrix, but have an elastic constant which does not equal that of the matrix. To this case the slab analogy cannot be applied without special modifications which will be discussed in a later publication.

The coefficients of proportionality for Figs. 10–16 were taken the same as for Figs. 4–7. The stress fields calculated from the Moiré fringes seem to be very reasonable. If the circular hole in Figs. 10 and 12 is assumed to be a vacancy in a crystal, the pictures show the stress relief of the edge dislocation due to a vacancy in the neighborhood of the dislocation. It may be possible to find the most stable position of the vacancy in the neighborhood of the dislocation, if the strain energy is calculated for the various positions of the vacancy. This strain energy can be calculated from the potential energy supplied to the analogous slab.

The example shown in Figs. 13–16 may be useful in the study of fracture initiation or migration. Zener [13] suggested a possibility of the initiation of a micro-crack at the root of the piled-up edge dislocations. The direction of the crack in this experiment was taken along the y'-axis with an angle of 70·5° to the x-axis and the two dislocations are piled-up along the x-axis. Stroh [14] found this angle as the direction where the maximum tensile stress is acting, and also calculated a similar stress field when many dislocations are piled-up and a crack was initiated at the root of the leading dislocation. Stroh had to make several assumptions in his calculation, which become unnecessary if the slab analogy is applied.

As a general conclusion, it can be said that the slab analogy presented in this paper gives a useful method for the two-dimensional stress analysis in the field of micro-mechanics, provided that errors sometimes as large as 10 per cent are admissible. Some of the errors are due to the creep and non-uniform sheet thickness of Plexiglas, both presumably being capable of improvement by use of alternative materials.

Another source of error is presented by a finite rather than infinite extent of the model slab leading to discrepancies of the type shown at large y in Figs. 5 and 11.

Acknowledgement—The research upon which this paper was based was supported by the Advanced Research Projects Agency of the Department of Defense, through the Northwestern University Materials Research Center.

REFERENCES

[1] A. TIMPE, *Z. Math. Phys.* **52,** 348 (1905).
[2] K. WIEGHARDT, *Mitt. ForschArb. Ingenieurw.* **49,** 15 (1908).
[3] V. P. JENSEN, *Experimental Determination of Non-linear Distribution of Stress by Slab Analogy, with Application to Hoover Dam,* University of Illinois (1931).
[4] H. CRANTZ, *Ingen.-Arch.* **10,** 159 (1939).
[5] R. D. MINDLIN, *Quart. appl. Math.* **4,** 279 (1946).
[6] R. D. MINDLIN and M. G. SALVADORI, *Handbook of Experimental Stress Analysis* (Edited by M. Hetenyi) pp. 700–827. John Wiley, New York (3rd edition) (1954).
[7] O. C. ZIENKIEWICZ and C. CRUZ, *Int. J. Mech. Sci.* **4,** 285 (1962).
[8] J. G. BOUWKAMP, *Experimental Mechanics,* (Edited by R. E. Rossi) pp. 195–219. Pergamon Press, Oxford (1963).
[9] F. K. LIGTENBERG, *Proc. Soc. exp. Stress Anal.* **12,** 83 (1955).
[10] W. BRADLEY, *Proc. Amer. Soc. civ. Engrs* **85,** No. EM4, 77 (1959).
[11] J. DUNDURS and T. MURA, *J. Mech. Phys. Solids* **12,** 177 (1964).
[12] R. PEIERLS, *Proc. Phys. Soc.* **52,** 34 (1940).
[13] C. ZENER, *Fracturing of Metals,* pp. 3–31. Amer. Soc. Metals (1948).
[14] A. N. STROH, *Proc. Roy. Soc.* **A223,** 404 (1954).

(*Received* 24 *June* 1964)

Zusammenfassung—Ebene Spannungsfelder in Kristallen, erzeugt durch Randversetzungen, Vakanzen, Prezipitationen, Risse und deren Kombinationen, werden experimentell bestimmt durch Anwendung der Analogie zwischen der Airy'schen Spannungsfunktion in einer Scheibe und der Durchbiegung einer Platte. Die Resultate stimmen ziemlich gut überein mit denen, die theoretisch erhalten wurden. Es ist somit festgestellt worden, dass komplizierte Probleme der Spannungsberechnung auf dem Gebiete der Mikromechanik mit den in dieser Arbeit vorgeschlagenen Methoden gelöst werden können.

Абстракт—Получены экспериментально двумерные поля в кристаллах, образованные вследствие дислокаций на краях, или из за пустот, выпадения, растрескивания или их комбинаций, употребляя аналогию плиты, между функцией напряжения Айри в тонкой пластинке и прогибом в плите. Эти результаты согласуются достаточно хорошо с теоретическими результатами. Таким образом найдено, что некоторые сложные проблемы в анализе напряжений в области микромеханики могут быть разрешены посредством метода, предложенного в этой работе.